International Journal of Control, Automation, and Systems (2011) 9(6):1154-1163
DOI 10.1007/s12555-011-0617-1

Modeling and Neuro-Fuzzy Adaptive Attitude Control for Eight-Rotor MAV

Xiangjian Chen, Di Li, Yue Bai, and Zhijun Xu*

Abstract: This paper focuses on modeling and intelligent control of the new Eight-Rotor MAV which is used to solve the problem of low coefficient proportion between lift and gravity for Quadrotor MAV. The dynamical and kinematical modeling for the Eight-Rotor MAV was developed which has never been proposed before. Based on the achieved dynamic modeling, two types of controller were presented. One type, a PID controller is derived in a conventional way with simplified dynamics and turns out to be quite sensitive to sensor noise as well as external perturbation. The second type controller is the Neuro-Fuzzy adaptive controller which is composed of two type-II fuzzy neural networks (T-IIFNNs) and one PD controller: The PD controller is adopted to control the attitude, one of the T-IIFNNs is designed to learn the inverse model of Eight-Rotor MAV on-line, the other one is the copy of the former one to compensate for model errors and external disturbances, both structure and parameters of T-IIFNNs are tuned on-line at the same time, and then the stability of the Eight-Rotor MAV closed-loop control system is proved using Lyapunov stability theory. Finally, the validity of the proposed control method has been verified through real-time experiments. The experimental results show that the performance of Neuro-Fuzzy adaptive controller performs very well under sensor noise and external disturbances, and has more superiority than traditional PID controller.

Keywords: Dynamical modeling of eight-rotor MAV, Lyapunov stability theorem, neuro-fuzzy adaptive controller, PID, Type-II fuzzy nerual network.

1. INTRODUCTION

Recently, researches on Micro Aerial Vehicles (MAVs) have been vigorously being performed for calamity observation, spraying agricultural chemicals, military purpose such as reconnaissance, monitoring, and communication etc. Moreover, the technology of the MAVs is getting faster according to the rapid progress of electronic and computer technology. MAVs can be operated on wide area regardless of the effect of ground configuration. The merit of MAVs is maximized for the practical use in the places where it is dangerous and difficult to approach. Further, MAVs are much cheaper and safer in dangerous tasks than piloted aircrafts.

MAV are classified into two categories, fixed and rotary wing types. The rotary wing type MAVs are more advantageous than the fixed wing type ones in the sense of VTOL(Vertical Take-off and Landing), omni-directional flying, and hovering performances. Rotary wing type MAVs are classified into quad-rotor type (QRT), co-axial helicopter, and helicopter etc. QRT MAVs have the simplest mechanical structure among them, and the quadrotor we consider is an underactuated system with six outputs and four inputs, and the states are highly coupled. To deal with this problem, many modeling approaches have been presented [1,2] and various control methods proposed [3-7]. Bouabdallah *et al*. presented PID vs. LQ Control Techniques Applied to an Indoor MicroQuadrotor [3]. Tayebi *et al*. studied attitude stablilization of a VIOL quadrotor aircraft [4]. Another PD control method was proposed by Erginer *et al.* [5]. Feedback Linearization vs. Adaptive Sliding Mode Control for a Quadrotor Helicopter was implemented by Lee. Daewon *et al.* [6]. A new robust adaptive-fuzzy control method applied to quadrotor helicopter stabilization was proposed by Coza *et al.* [7].

Of course, the whole purpose of the MAV is to carry a payload. For the moment, the primary mission assigned to MAVs is aerial observation and surveillance. MAVs are obviously an advantageous solution for missions where a live crew offers no real benefits, or where the risk are too high. In general, for MAVs to carry out the missions under consideration, all aspects of the system will have to be improved: the vehicle itself, payloads and especially sensors, transmission systems, onboard intelligence, and so on.

We introduce, in this paper, one configuration of a multi rotor helicopter composed of eight rotors, which is used to solve the problem of low coefficient proportion between lift and gravity of Quadrotor MAV. The main characteristics of the configurations are that increased payload capacity, quiet-efficient, stability in the wind

Manuscript received March 22, 2010; revised May 11, 2011; accepted June 29, 2011. Recommended by Editorial Board member Young Jae Lee under the direction of Editor Jae Weon Choi.

This work was supported by National Natural Science Foundation of China NSFC 50905174.

Xiangjian Chen and Di Li are with Chang Chun Institute of Optics Fine Mechanics and Physics, Chinese Academy of Sciences, China (e-mails: cxj831209@163.com, lidi19821111@163.com).

Yue Bai and Zhijun Xu are with Chinese Academy of Sciences, China (e-mails: baiyue@ciomp.ac.cn, xuzj538@ciomp.ac.cn).

* Corresponding author.

and damage tolerance. The dynamical model is presented, to validate the model we introduce an intelligent control strategy and apply it in real-time experiences. The control strategy is based on Neuro-Fuzzy adaptive controller, Neuro-Fuzzy has been used in a lot of successful applications [8-13], such as Spooner *et al*. [8] and Ordonez *et al*. [9] proposed the combination of fuzzy systems and neural network to make the adaptive control systems. Melin *et al.* used neuro–fuzzy–fractal approach to adaptive control one model-based non-linear dynamic plants [10]. Lou *et al*. used neuro-fuzzy method to modeling and adaptive control the mechanism [11]. Melin *et al*. used neuro–fuzzy–genetic approach to control of complex electrochemical systems [12]. Er *et al*. designed dynamic fuzzy neural networks controller for a SCARA and make the real-time implementation [13]. But which is based on type-I fuzzy sets. With the higher control accuracy requirements, type-II fuzzy neural network [14-17] is developed recently which has better performances than type-I fuzzy neural network. Such as system identification by using type-2 fuzzy neural network was developed by Lee *et al*. [14], and Wang studied dynamic optimal training for interval type-2 fuzzy neural networks [15]. Double axes motion control system and dynamic time-varying system identification with type-II fuzzy neural networks were designed by Chen *et al*. [16,17]. This paper is to apply type-II fuzzy neural networks to control the attitude of the Eight-Rotor MAV. So robust adaptive attitude controller proposed which is composed of two type-II fuzzy neural networks (T-IIFNNs) and one PD controller: PD controller is to control the attitude; one of the T-IIFNNs is used to learn the inverse model of Eight-Rotor MAV on-line; the other one is the copy of the former one to compensate for model errors, sensor noises and orther external disturbances.

This paper is structured as followings: In Section 2, the flight theory of the Eight-Rotor MAV is presented. In Section 3, super characteristics of Eight-Rotor MAV than QuadRotor MAV are described. In Section 4 we develop the mathematical nonlinear model of the Eight-Rotor MAV. The flight control algorithm is given in Section 5, which is also devoted to the stability analysis of the control scheme. Platform description and some experiences are given in Section 6 and Section 7 contains concluding remarks.

2. FLIGHT THEORY OF EIGHT-ROTOR MAV

The Eight-Rotor is very well modeled with eight rotors in a cross configuration. This cross structure is quite thin and light, however it shows robustness by linking mechanically the motors. Each propeller is connected to the motor through the reduction gears. All the propellers axes of rotation are fixed and parallel. These considerations point out that the structure is quite rigid and the only things that can vary are the propeller speeds. Neither the motors nor the reduction gears are fundamental because the movements are directly related just to the propellers velocities can be seen in Table 1 and Fig. 1, where $\Omega_i (i = 1, 2, \cdots, 6)$ respects to speed of Rotor *i*th. This can be expanded to move the Eight-Rotor platform at any combination of yaw, roll, and pitch. Because the Eight-Rotor can be controlled by simply varying the speed of 8 motors, it is a very mechanically simple platform.

Table 1. Flight theory for Eight-Rotor MAV.

$\Omega_1 + \Omega_2 = \Omega_3 + \Omega_4 =$ $\Omega_5 + \Omega_6 = \Omega_7 + \Omega_8$	Even, Upward Thrust $\Rightarrow$ No pitch or roll Torques generated by rotors cancel $\Rightarrow$ No yaw
$(\Omega_5 + \Omega_6 + \Omega_1 + \Omega_2) =$ $(\Omega_3 + \Omega_4 + \Omega_7 + \Omega_8)$ $(\Omega_1 + \Omega_2) > (\Omega_5 + \Omega_6)$ $(\Omega_3 + \Omega_4) = (\Omega_7 + \Omega_8)$	Torques cancelled $\Rightarrow$ No yaw More thrust at Rotors 1,2 than Rotors 5,6 $\Rightarrow$ Pitch Thrust at Rotors 3,4=Thrust at Rotors 7,8 $\Rightarrow$ No roll
$(\Omega_5 + \Omega_6 + \Omega_1 + \Omega_2) =$ $(\Omega_3 + \Omega_4 + \Omega_7 + \Omega_8)$ $(\Omega_7 + \Omega_8) > (\Omega_3 + \Omega_4)$ $(\Omega_1 + \Omega_2) = (\Omega_5 + \Omega_6)$	Torques cancelled $\Rightarrow$ No yaw More thrust at Rotors 7,8 than Rotors 3,4 $\Rightarrow$ Roll Thrust at Rotors 1,2=Thrust at Rotors 5,6 $\Rightarrow$ No pitch
$(\Omega_3 + \Omega_4 + \Omega_7 + \Omega_8) >$ $(\Omega_5 + \Omega_6 + \Omega_1 + \Omega_2)$ $(\Omega_7 + \Omega_8) = (\Omega_3 + \Omega_4)$ $(\Omega_1 + \Omega_2) = (\Omega_5 + \Omega_6)$	More torque generated by Rotors3,4,7,8 than Rotors 5,6,1,2 $\Rightarrow$ Yaw Thrust at Rotors 7,8=Thrust at Rotors 3,4 $\Rightarrow$ No pitch Thrust at Rotors 1,2=Thrust at Rotors 5,6 $\Rightarrow$ No roll

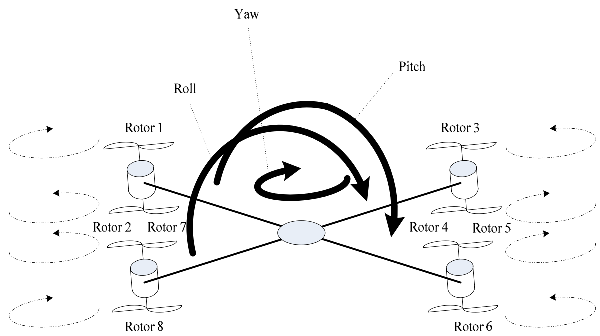

Fig. 1. Flight theory of Eight-Rotor MAV.

3. SUPERIORITY RELATIVE TO QUADROTOR MAV

3.1. Increased payload capability

The Eight-Rotor MAV has a payload capacity of approximately1 kilogram, the largest of all the Quadrotor MAV with the same mechanical size. To achieve this, the Eight-Rotor uses an innovative tilted eight-rotor design. The eight rotors are arranged as four counter-rotating offset pairs mounted at the ends of four carbon fiber arms. The four sets of matched counter rotating rotor blades provide differential thrust from four equally spaced points, which allows the Eight-Rotor MAV to maneuver with precision and speed. The larger Eight-Rotor also provides improved performance in the wind due to its larger size and weight. Using the offset layout of the rotors increases the thrust without increasing the size of the footprint, and naturally eliminates the loss of efficiency due to torque compensation.

3.2. Quiet and efficient

The Eight-Rotor MAV features a unique design that minimizes thrust lost to sound output. The rotor blades have been designed for maximum efficiency while naturally producing less turbulence when spinning. The motors are direct drive which reduces moving parts and eliminates and gear box noise. While hovering, the Eight-Rotor produces less than approximately 78dB of sound at one meter.

3.3. Increased stability in the wind

The Eight-Rotor UAV weighs approximately 1700 grams (60 oz) and has the increased thrust of 8 counter-rotating rotors which allows it to be much more stable in windy conditions. The larger size and weight of the Eight-Rotor make it a very stable helicopter to fly.

3.4. Damage tolerance

The frame of the Eight-Rotor is built from high quality military grade carbon fibre making it one of the most durable electric helicopters on the market today. Carbon fibre is impervious to rust and does not decay making it an excellent choice for strong light weight constructions. In order to meet the demands placed on a MAV, the Eight-Rotor has been designed with durability in mind. Making use of strong light weight materials like carbon fibre and glass-filled injected nylon plastic parts, the Eight-Rotor is able to stand up to a significant amount of stress during flight. The frame has been designed to be rigid in order to improve flight response while at the same time able to absorb vibration.

Eight-Rotor could remain stable flighting while some of the eight rotors broken. If one rotor is broken, another in pairs will compensate the lift reduced caused by the broken rotor.

The individual arms on the Eight-Rotor can be replaced rather than having to replace the entire frame making it less costly to repair should repairs be needed. Every rotor on the Eight-Rotor is simple and easy to replace making it a snap to change them in the field should the need arise.

4. EIGHT-ROTOR MAV DYNAMIC MODELLING

The first step before control development is an adequate dynamic system modeling. Let us consider two frames have to be defined: the earth inertial frame (E-frame) [10]; the body-fixed frame (B-frame).

Equation (1) describes the kinematics of a generic 6 degree of freedom rigid-body:

$$\dot{\eta} = \begin{bmatrix} R & 0_{3\times3} \\ 0_{3\times3} & T \end{bmatrix} v, \tag{1}$$

where the η means orientation and position of Eight-Rotor MAV with respect to inertial reference frame; while the v means the linear and angular velocities of orientation and position of Eight-Rotor MAV with respect to the body-fixed frame, x, y, z represents the linear positions, and ϕ, θ, ψ represents the roll, pitch and yaw angles in inertial reference frame respectively. η and v are shown in

$$\eta = [x \quad y \quad z \quad \phi \quad \theta \quad \psi]^T, \tag{2}$$

$$v = [u \quad v \quad w \quad p \quad q \quad r]^T. \tag{3}$$

The notation $0_{3\times3}$ means a sub-matrix with dimension 3 times 3 filled with all zeros while the rotation R and the transfer T matrices are defined according to

$$R = \begin{bmatrix} c\psi c\theta & -s\psi c\phi + c\psi s\phi s\theta & s\psi s\phi + c\psi s\theta c\phi \\ s\psi c\theta & c\psi c\iota + s\psi s\phi s\theta & -c\psi s\phi + s\psi s\theta c\phi \\ -s\theta & c\theta s\phi & c\theta c\phi \end{bmatrix}, \tag{4}$$

$$T = \begin{bmatrix} 1 & s\phi \tan\theta & c\phi \tan\theta \\ 0 & c\phi & -s\phi \\ 0 & s\phi/c\theta & c\phi/c\theta \end{bmatrix}. \tag{5}$$

The dynamics of a generic 6 degree of freedom rigid-body takes into account the mass of the body m and its inertia matrix I which is calculated in this work. The dynamics is described by

$$\begin{bmatrix} mI_{3\times3} & 0_{3\times3} \\ 0_{3\times3} & I \end{bmatrix} \begin{bmatrix} v \\ \omega \end{bmatrix} + \begin{bmatrix} \omega \times mV \\ \omega \times I\omega \end{bmatrix} = \begin{bmatrix} F^B \\ \tau^B \end{bmatrix}, \tag{6}$$

where the notation $I_{3\times3}$ means a 3 times 3 identity matrix. V is the Eight-Rotor linear speed vector while ω is the Eight-Rotor angular speed. In addition, F^B is the Eight-Rotor forces vector and τ^B is the quadrotor torques vector with respect to B-frame. A generalized force vector A can be defined according to

$$\Gamma = [F^B \quad \tau^B] = [F_x \quad F_y \quad F_z \quad \tau_x \quad \tau_y \quad \tau_z]^T. \tag{7}$$

Hence the last vector contains specific information about its dynamics. Γ can be divided in three components according to the nature of the Eight-Rotor contributions.

The first contribution is the gravitational vector $G_B(\xi)$ given from the acceleration due to gravity g. It's easy to understand that it affect just the linear and not the angular equations since it's a force and not a torque. (8) shows the transformations to get $G_B(\xi)$.

$$G_B = \begin{bmatrix} F^B \\ 0_{3\times1} \end{bmatrix} = \begin{bmatrix} R^{-1}F^E \\ 0_{3\times1} \end{bmatrix} = \begin{bmatrix} mgs\theta \\ -mgc\theta s\phi \\ -mgc\theta s\phi \\ 0 \\ 0 \\ 0 \end{bmatrix}, \tag{8}$$

where F^B the gravitational force is vector with respect to B-frame and F^E is that one with respect to E-frame.

Furthermore, since R is an orthogonal normalized matrix, its inverted R^{-1} is equal to the transposed one R^T.

The second contribution takes into account the gyroscopic effects produced by the propeller rotation. Since four of them are rotating clockwise and the other four counter clockwise. There is a overall rotor speeds is not equal to zero. If, in imbalance when the algebraic sum of the addition, the roll or pitch rates are also different than zero, the Eight-Rotor experiences a gyroscopic torque according to (9). $O_B(v)$ is the gyroscopic propeller matrix and J_T is the total rotational moment of inertia around the propeller axis calculated in the next section. It's easy to see that the gyroscopic effects produced by the propeller rotation are just related to the angular and not the linear equations.

$$O_B(v)\Omega = \begin{bmatrix} -\sum_{i=1}^{8} J_T \begin{bmatrix} 0_{3\times1} \\ \omega \times \begin{bmatrix} 0 \\ 0 \\ 0 \end{bmatrix} \end{bmatrix} (-1)^i \Omega_i \end{bmatrix} \tag{9}$$

The third contribution takes into account the forces and torques directly produced by the main movement inputs. From aerodynamics consideration, it follows that both forces and torques are proportional to the squared propellers' speed. Therefore the movement matrix E_B is multiplied by Ω^2 to get the movement vector U_B. Equation (10) shows the action of the movement vector on the Eight-Rotor helicopter dynamics.

$$U_B = \begin{bmatrix} 0 \\ 0 \\ b\begin{pmatrix} (\Omega_1+\Omega_2)^2 + (\Omega_3+\Omega_4)^2 \\ +(\Omega_5+\Omega_6)^2 + (\Omega_7+\Omega_8)^2 \end{pmatrix} \\ dl\left((\Omega_1+\Omega_2)^2 - (\Omega_5+\Omega_6)^2\right) \\ dl\left((\Omega_7+\Omega_8)^2 - (\Omega_3+\Omega_4)^2\right) \\ dl\begin{pmatrix} \left((\Omega_7+\Omega_8)^2 + (\Omega_3+\Omega_4)^2\right) \\ -\left((\Omega_1+\Omega_2)^2 - (\Omega_5+\Omega_6)^2\right) \end{pmatrix} \end{bmatrix}, \tag{10}$$

where l is the distance between the center of the Eight-Rotor and the center of a propeller, b means the square of motor speed-lift scaling factor, d means force-moment scaling factor, U_1, U_2, U_3 and U_4 are the movement vector components. Their relation with the propellers' speeds comes from aerodynamic calculus. Therefore all the movements have a similar expression and are easier to control. It is possible to describe the Eight-Rotor dynamics considering these last three contributions according to

$$\Gamma = G_B(\xi) + O_B(v)\Omega + E_B\Omega^2. \tag{11}$$

Equation (12) shows the previous expression not in a matrix form, but in a system of equations

$$\begin{cases} m\ddot{x} = (s\psi s\phi + c\psi c\theta)U_1 \\ m\ddot{y} = (-c\psi s\phi + s\theta s\psi c\phi)U_1 \\ m(\ddot{z}+g) = c\theta c\phi U_1 \\ I_x\dot{\omega}_x + (I_z - I_y)\omega_y\omega_x = U_2 \\ I_y\dot{\omega}_y + (I_x - I_z)\omega_z\omega_x = U_3 \\ I_z\dot{\omega}_z = U_4, \end{cases} \tag{12}$$

where the propellers' speed inputs are given through

$$\begin{cases} U_1 = b((\Omega_1+\Omega_2)^2 + (\Omega_3+\Omega_4)^2 \\ \qquad +(\Omega_5+\Omega_6)^2 + (\Omega_7+\Omega_8)^2) \\ U_2 = dl((\Omega_1+\Omega_2)^2 - (\Omega_5+\Omega_6)^2) \\ U_3 = dl((\Omega_7+\Omega_8)^2 - (\Omega_3+\Omega_4)^2) \\ U_4 = dl(((\Omega_7+\Omega_8)^2 + (\Omega_3+\Omega_4)^2) \\ \qquad -((\Omega_1+\Omega_2)^2 + (\Omega_5+\Omega_6)^2)). \end{cases} \tag{13}$$

The dynamics of the Eight-Rotor is well described in the previous section. However the most important concepts can be summarized in (12), (13). The first one shows how the Eight-Rotor accelerates according to the basic movement commands given. The second equation explains how the basic movements are related to the propellers' squared speed. The goal of the Eight-Rotor stabilization is to find those values of the motors' voltage which maintains the helicopter in a certain position required in the task. This process is also known as inverse kinematics and inverse dynamics. Unlike the direct ones, the inverses operations are not always possible and not always unique. For these reasons their consideration is much more complicated.

5. CONTROLLER DESIGN

5.1. PID controller

The Eight-Rotor dynamics must be simplified a lot to provide an easy inverse model which can be implemented in the control algorithms. Especially, the hovering control with $\phi \approx 0; \theta \approx 0$ can make the dynamics much simpler form like (14), and it is easy to design the controller. Now, let us consider following composite dynamic equations of motion:

$$\begin{bmatrix} m(\ddot{z}+g) \\ I_x\ddot{\phi} \\ I_y\ddot{\theta} \\ I_z\ddot{\psi} \end{bmatrix} + \Delta = \begin{bmatrix} U_1 \\ U_2 \\ U_3 \\ U_4 \end{bmatrix}, \tag{14}$$

where, the disturbance Δ is defined as:

$$\Delta = \begin{bmatrix} \delta_3 \\ \delta_4 + (I_z - I_y)\dot{\theta}\dot{\psi} \\ \delta_5 + (I_x - I_z)\dot{\psi}\dot{\phi} \\ \delta_6 \end{bmatrix} \tag{15}$$

and δ_i mainly comes from dynamic inconsistency, the

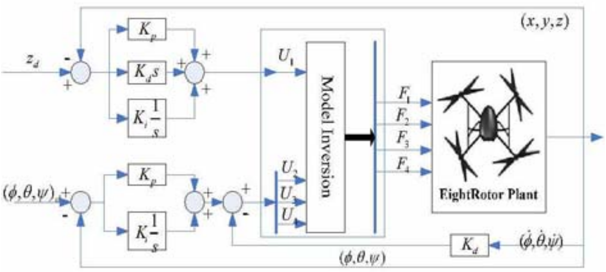

Fig. 2. PID controller for controlling position and attitude of Eight-Rotor MAV.

control algorithms for the position and attitude of the SixRotor MAV are designed based on PID controllers as shown in Fig. 2. The control inputs U_1 for controlling the position z of the Eight-Rotor with respect to the reference input z_d are designed as:

$$u_1 = K_{p1}[z_d - z] + K_{d1}\frac{d[z_d - z]}{dt} + K_{i1}\int_0^t [z_d - z]\,d\tau. \tag{16}$$

The control inputs $U_j\,(j = 2,3,4)$ for controlling the attitude (ϕ, θ, ψ) of the SixRotor with respect to the reference input ϕ_d, θ_d, ψ_d are designed as:

$$\begin{aligned} u_j &= K_{pj}[(\phi,\theta,\psi)_d - (\phi,\theta,\psi)] + K_{dj}(\dot{\phi},\dot{\theta},\dot{\psi}) \\ &\quad + K_{ij}\int_0^t [(\phi,\theta,\psi)_d - (\phi,\theta,\psi)]\,d\tau. \end{aligned} \tag{17}$$

The above control algorithms (16) and (17) control the position and angular of the MAV using sensor signals. The flight performance is not good in real flight because of the sensor noises and disturbances.

5.2. Neuro-Fuzzy adaptive controller

For the control purpose, it is more convenient to use the dynamic model in earth-fixed coordinate frame like below:

$$M_\eta(\eta)\ddot{\eta} + C_\eta(v,\eta)\dot{\eta} + g_\eta(\eta) = \tau_\eta + \tau_d, \tag{18}$$

where $\dot{\eta} = J(\eta)v; \ddot{\eta} = J(\eta)\dot{v} + \dot{J}(\eta)v$, and τ_d represents the external disturbance, the system matrices are defined as following:

$$\begin{aligned} &\mathrm{M}_\eta(\eta) = J^{-T}(\eta)MJ^{-1}(\eta), \\ &C_\eta(v,\eta) = 1/2\dot{M}_\eta(\eta), \\ &g_\eta(\eta) = J^{-T}(\eta)g(\eta), \\ &\tau_\eta(\eta) = J^{-T}(\eta)\tau, \end{aligned} \tag{19}$$

where

$$\mathrm{J}(\eta) = \begin{bmatrix} c\psi c\theta & -s\psi c\phi + c\psi s\theta s\phi & s\psi s\phi + c\psi c\phi s\theta & 0 & 0 & 0 \\ s\psi c\theta & c\psi c\phi + s\psi s\theta s\phi & -c\psi s\phi + s\psi s\phi c\theta & 0 & 0 & 0 \\ -s\theta & c\theta s\phi & c\theta c\phi & 0 & 0 & 0 \\ 0 & 0 & 0 & 1 & s\phi t\theta & c\phi t\theta \\ 0 & 0 & 0 & 0 & c\phi & -s\phi \\ 0 & 0 & 0 & 0 & s\phi/c\theta & c\phi/c\theta \end{bmatrix}^T. \tag{20}$$

For the moving base system which is not fixed in an inertial frame. We can derive the equations of motion in earth-fixed coordinate frame as followings:

$$\begin{cases} m\ddot{z} = c\theta c\phi u_1 - mg \\ M_2\ddot{\eta} + \frac{1}{2}\dot{M}_2\dot{\eta} = \begin{bmatrix} u_2 \\ u_3 c\phi - u_4 s\phi \\ -u_2 s\theta + u_3 c\theta s\phi + u_4 c\theta c\phi \end{bmatrix}, \end{cases} \tag{21}$$

where

$$M_2 = \begin{bmatrix} I_{xx} & 0 & -I_{xx}s\theta \\ 0 & I_{yy}c^2\theta + I_{zz}s^2\phi & (I_{yy} - I_{zz})c\phi c\theta s\phi \\ -I_{xx}s\theta & (I_{yy} - I_{zz})c\phi c\theta s\phi & I_{xx}s^2\theta + I_{yy}c^2\theta s^2\phi + I_{zz}c^2\theta c^2\phi \end{bmatrix} \tag{22}$$

and

$$\tau_\eta = [U_1 \quad U_2 \quad U_3 \quad U_4]^T. \tag{23}$$

The proposed control architecture on the target system based on Neuro-Fuzzy controller is shown in Fig. 3. The controller used here is dynamic type II fuzzy neural networks (T-IIFNN) [16,17] which have dynamic self-organizing structure, fast learning speed, good generalization, and better performance than type-I fuzzy neural network.

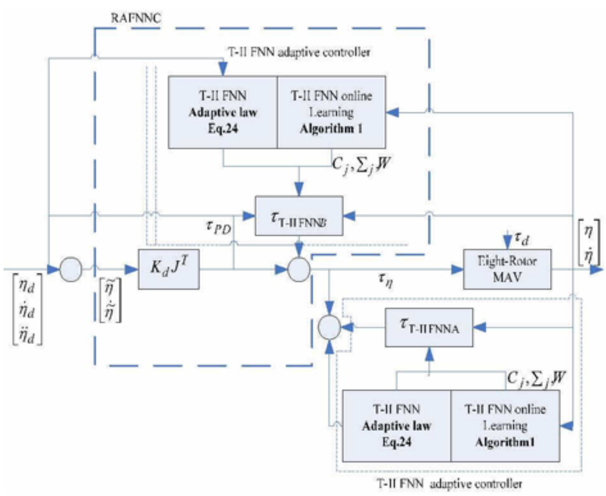

Fig. 3. Robust adaptive control system for Eight-Rotor MAV with Neuro-Fuzzy controller.

From Fig. 3, we can see that the control strategy is composed of two T-IIFNNs and one PD controller: the PD controller is used to control the attitude angles; the T-IIFNNs are employed to learn the inverse model of the Eight-Rotor and compensated for the model errors, external disturbance. The proposed control law is given by

$$\begin{aligned}\tau_\eta(\bar{\eta}) &= \tau_{T-IIFNN}(\bar{\eta} \mid W) + \tau_{PD} \\ &= \tau_{T-IIFNN}(\bar{\eta} \mid W) + K_d e \\ &= W^T \Phi(\bar{\eta}) + K_d e,\end{aligned} \tag{24}$$

where τ_η is the required control torque, $K_d e$ is the torque generated by the PD controller and $\tau_{T\text{–}IIFNN}$ is the torque generated by T-IIFNNs. The inverse Eight-Rotor model is obtained by T-IIFNs. With online learning, one of T-IIFNNs is trained during real-time control of the manipulator. The other one is a duplicate copy of the former one, but its structure and parameters will be further adjusted by the error signal τ_{PD} as the controller is in operation, which is to compensate for modeling errors and external disturbances τ_d.

The on-line learning algorithm 1 [15] used in the Fig. 3 has been shown in Fig. 4.

Algorithm 1: Constructing T-IIFNN via on-line structure and parameters learning with optimal learning rate concurrently. The flow chart for T-IIFNN with structure and parameters learning has been shown in Fig. 4.

5.3. Stability analysis

The adaptive law of W is designed as follows:

$$\dot{W}_i = k\Phi\bar{e}M_\eta b_i, \quad i = 1, \cdots, m, \tag{25}$$

where m is the number of input variables of the MAV system or the output variables of the self-organizing interval type-II fuzzy neural networks, M is the symmetric positive definite matrix which is selected by user. Guaranteeing the stability of the control system, the parameters of the self-organizing interval type-II fuzzy neural networks must be bounded, which could be done if the consequent parameters W be bounded. Define the constraint set Γ as shown in (26) for W expressed as (25), (26) is expressed as following:

$$\Gamma = \{\|w_i\| \le \|w_0\|\}, \quad i = 1 \cdots m. \tag{26}$$

The adaptation law can be rewritten as follows:

$$\dot{w}_i = \begin{cases} k\Phi\bar{e}^T M_\eta b & if(\|w_i\| < \|w_i(0)\|) or(\|w_i\| < \|w_i(0)\| \\ & and w_i^T \Phi\bar{e}^T M_\eta b_i \le 0 \\ k(I - \dfrac{w_i w_i^T}{\|w_i\|^2})\Phi\bar{e}^T M_\eta b & if(\|w_i\| = \|w_i(0)\| \\ & and w_i^T \Phi\bar{e}^T M_\eta b_i > 0). \end{cases} \tag{27}$$

Theorem 1: If the initial values of the weights $w_i(0) \in \Gamma$, the adaptation law guarantees $w_i(t) \in \Gamma$, $\forall t > 0$. The proof can be found in the reference [18].

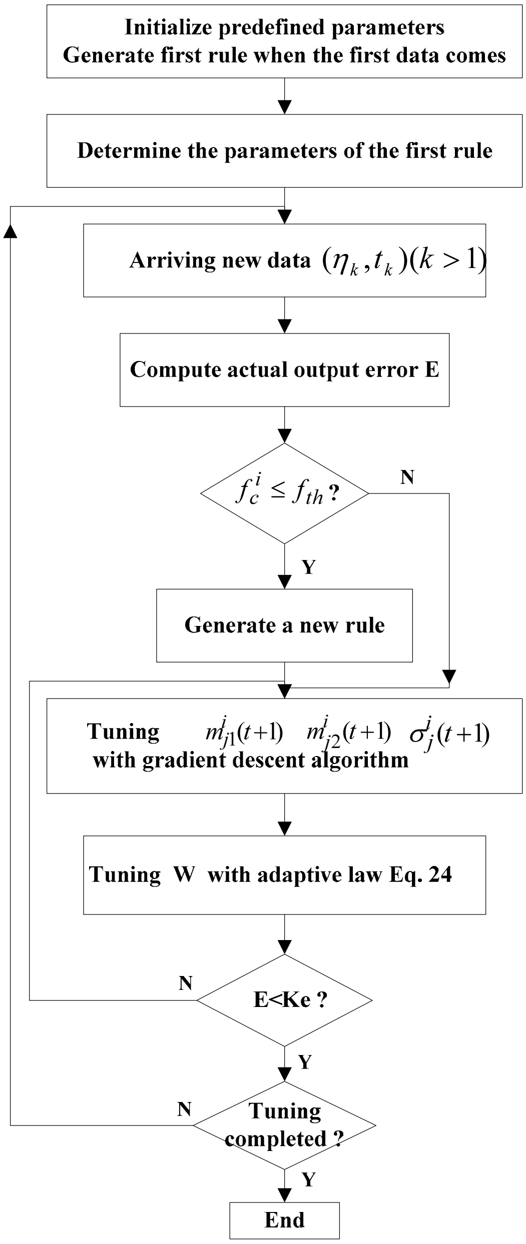

Fig. 4. Flow chart of proposed Algorithm 1.

Theorem 2: Consider the MAV dynamic system represented by (18). If the adaptive control law of (24) is applied, the asymptotic stability is guaranteed.

Proof: We consider the following Lyapunov function candidate as follows:

$$V(t) = \frac{1}{2}\bar{\dot{e}}M_\eta\bar{e} + \frac{1}{2}\bar{e}M_\eta\bar{\dot{e}} - k^{-1}tr[(W^* - W)^T(W^* - W)]. \tag{28}$$

Under Condition 1, taking the derivative of the Lyapunov function as follows:

$$\begin{aligned}\dot{V}(t) &= \frac{1}{2}\dot{\bar{e}}^T M_\eta \bar{e} + \frac{1}{2}\bar{e}^T M_\eta \dot{e} - k^{-1}tr[(W^* - W)^T \dot{W}] \\ &= -\frac{1}{2}\bar{e}^T K_d \bar{e} + \bar{e}^T J(\eta)K(W^* - W)^T \Phi\end{aligned} \tag{29}$$

$$
\begin{aligned}
&-k^{-1}tr[(W^*-W)^T\dot{W} \\
&=-\frac{1}{2}\overline{e}^T K_d\overline{e}+\overline{e}^T J(\eta)K(W^*-W)^T\Phi \\
&-tr[\overline{e}^T J(\eta)K(W^*-W)^T\Phi] \\
&=-\frac{1}{2}\overline{e}^T K_d e\le 0.
\end{aligned}
$$

Under condition 2, and assuming that $w_i^*\in\Gamma$, then:

$$
\begin{aligned}
\dot{V}(t)&\le -e^T K_d e+tr\left\{\tilde{W}^T\left[r(J^{-1}e)^T+k^{-1}\dot{\tilde{W}}\right]\right\} \\
&=-e^T K_d e+tr\left\{\tilde{W}^T\left[\frac{w_1w_1^T}{\|w_1\|}rb_1,\frac{w_2w_2^T}{\|w_2\|}rb_2,\right.\right. \\
&\qquad\left.\left.\dots,\frac{w_Nw_N^T}{\|w_N\|}rb_N\right]\right\} \qquad (30) \\
&=-e^T K_d e+\sum_{K=1}^{N}[(w_k^*-w_k)^T\frac{w_kw_k^T}{\|w_k\|}rb_k] \\
&=-e^T K_d e+\sum_{K=1}^{N}[(\frac{(w_k^*)^T w_k}{\|w_k\|^2}-1)^T w_k^T rb_k] \\
&=-e^T K_d e\le 0.
\end{aligned}
$$

Since $w_i^*\in\Gamma$ and $\frac{w_i^{*T}w_i}{\|w_i\|^2}\le 1$, then:

$$\dot{V}(t)\le -\frac{1}{2}\overline{e}^T K_d\overline{e}\le 0.$$

Therefore, global stability is guaranteed by the Lyapunov theorem. As a result, the control system is asymptotically stable. Moreover, the tracking error of the system will converge to zero.

6. EXPERIMENTAL RESULTS

6.1. Experimental setup

The schematic view of the aerial control platform using TMS320F2812 has been shown in Fig. 5. The Eight-Rotor MAV has four blades driven by eight BLDC motors mounted at each end of the body frame. The Encoders were used for measuring the speed of each motor. The INS data are updated at 5 Hz and the static pressure sensor measures are provided at a rate of 50 Hz, the low-cost IMU which outputs raw data from 3 accelerometers, 3 gyro meters and 3 magnetometers at the need of 50 Hz to the flight control computer which receives all these sensor data through an RS-232 serial port. The on-board flight control computer is TMS320F2812 (DSP) which runs at 29.4M Hz, with 512k flash memory, including eight serial ports, eight channels with programmable gains, 24-bit analog input, six programmable Pulse Width Modulation (PWM) outputs, and supports floFating point calculations.

For avoiding signal interference between sensor signals and the motors PWM, two independent power

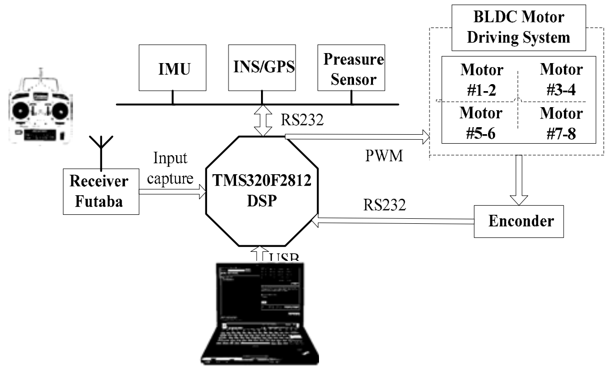

Fig. 5. Schematic view of aerial control platform using TMS320F2812.

supplies were supplied. One battery is used to feed the eight electric motors which are controlled using PWM, the other battery is used to feed microcontroller and the sensors, and by adequate grounding, the interference is reduced largely.

6.2. Experimental results

Real-time experiment results are presented in this section to validate the performance of the Eight-Rotor MAV. The control gains of equations were adjusted in practice to obtain a fast MAV response but avoiding mechanical oscillations as much as possible. The parameters were also chosen in such a way that the MAV attitude remains very close to a desired point.

Owing to the highly complex structure of the T-IIFNN, the computational load is quite heavy in the training and reasoning process. For the reason, it is necessary to simplify the control system for real-time control. Furthermore, fast response is imperative in order to deal with the real-time tracking with good control performance. The calssical fuzzy inference mechanism with three fuzzy inference rules is adopted. Each rule has two antecedent parts and one consequent part:

$$
\begin{aligned}
&R_1: IF\ x_1^1\ is\ \tilde{M}_1^1,\ and\ x_2^1\ is\ \tilde{M}_2^1, \\
&\quad THEN\ y_1\ is\ [w_{R1}^4, w_{L1}^4] \\
&R_2: IF\ x_1^1\ is\ \tilde{M}_1^2,\ and\ x_2^1\ is\ \tilde{M}_2^2, \\
&\quad THEN\ y_1\ is\ [w_{R2}^2, w_{L2}^4] \\
&R_3: IF\ x_1^1\ is\ \tilde{M}_1^3,\ and\ x_2^1\ is\ \tilde{M}_2^3, \\
&\quad THEN\ y_1\ is\ [w_{R3}^4, w_{L3}^4]
\end{aligned}
$$

In addition, T-II MFs and the weighting interval set are initialized as follows:

$$
\begin{aligned}
&\overline{m}_{11\theta}=0.3, && \overline{m}_{12\theta}=0.1, && \overline{m}_{13\theta}=0.6, \\
&\overline{m}_{21\theta}=0.3, && \overline{m}_{22\theta}=0.1, && \overline{m}_{23\theta}=1.6, \\
&\underline{m}_{11\theta}=-0.5, && \underline{m}_{12\theta}=-0.2, && \underline{m}_{13\theta}=-0.2, \\
&\underline{m}_{21\theta}=-1.5, && \underline{m}_{22\theta}=-0.2, && \underline{m}_{23\theta}=-0.2, \\
&\overline{m}_{11\phi}=0.6, && \overline{m}_{12\phi}=0.8, && \overline{m}_{13\phi}=1.2, \\
&\overline{m}_{21\phi}=0.3, && \overline{m}_{22\phi}=0.7, && \overline{m}_{23\phi}=1.4,
\end{aligned}
$$

$\underline{m}_{11\phi} = -1.7,\quad \underline{m}_{12\phi} = -0.2,\quad \underline{m}_{13\phi} = -0.1,$

$\underline{m}_{21\phi} = -1.3,\quad \underline{m}_{22\phi} = -0.4,\quad \underline{m}_{23\phi} = -0.2,$

$\overline{m}_{11\psi} = -0.1,\quad \overline{m}_{12\psi} = 0.3,\quad \overline{m}_{13\psi} = 0.9,$

$\overline{m}_{21\psi} = -0.3,\quad \overline{m}_{22\psi} = 0.2,\quad \overline{m}_{23\psi} = 1.2,$

$\underline{m}_{11\psi} = -0.3,\quad \underline{m}_{12\psi} = 0.1,\quad \underline{m}_{13\psi} = 0.5,$

$\underline{m}_{21\psi} = -0.6,\quad \underline{m}_{22\psi} = -0.1,\quad \underline{m}_{23\psi} = 0.6,$

$\sigma_{11\theta} = 5.2,\quad \sigma_{12\theta} = 7.5,\quad \sigma_{13\theta} = 3.5,$

$\sigma_{21\theta} = 4.6,\quad \sigma_{22\theta} = 5.5,\quad \sigma_{23\theta} = 6.3,$

$\sigma_{11\phi} = 5.6,\quad \sigma_{12\phi} = 2.5,\quad \sigma_{13\phi} = 4.6,$

$\sigma_{21\phi} = 3.2,\quad \sigma_{22\phi} = 5.5,\quad \sigma_{23\phi} = 6.5,$

$\sigma_{11\psi} = 1.2,\quad \sigma_{12\psi} = 2.2,\quad \sigma_{13\psi} = 2.3,$

$\sigma_{21\psi} = 1.8,\quad \sigma_{22\psi} = 1.5,\quad \sigma_{23\psi} = 3.1,$

$[w_{R1}^4, w_{L1}^4] = [-0.25, -5.36],$

$[w_{R2}^4, w_{L2}^4] = [-0.56, -6.53],$

$[w_{R3}^4, w_{L3}^4] = [-0.45, -1.24],$

$[w_{R1}^4, w_{L1}^4] = [-0.55, -2.66],$

$[w_{R2}^4, w_{L2}^4] = [-0.83, -4.35],$

$[w_{R3}^4, w_{L3}^4] = [-0.59, -7.24].$

All the parameters shown above are obtained by using initial formation. In the initial formation, the initial values of the network parameters are chosen randomly, and accurate tracking performance is obtained after 0.5 second online learning of the T-IIFNN using the adaptive learning Algorithm 1 shown in Fig. 4. Then, all the network parameters of the T-IIFNN after learning are saved for initial formation. After that, the control performance of the proposed Neuro-Fuzzy adaptive controller is investigated with the initial formation in the experimentation.

In the experiment, the Eight-Rotor was stabilized at hover applying the proposed control strategy, we have obtained an acceptable behavior which is shown in Fig. 6. The control objective is to make the MAV stablize the posture of Eight-Rotor to zero with the initial value are $\phi = -10^\circ$, $\theta = 7-30^\circ$, $\psi = -25^\circ$, $\dot{\phi} = \dot{\theta} = \dot{\psi} = 0^\circ$.

The experimental data returned by wireless communication subsystem and recorded through computer. Taking into account real-time control requirements, the experimental results are shown in Fig. 6. While Fig. 7 shows the results by using the PID control, which used to make a contrast with the Neuro-Fuzzy adaptive controller.

PID controllers are efficient in single-loop feedback control; however, classical control techniques do not address the issue of coupling exhibited by multi-variable systems such as the Eight-Rotor MAV. The results form comparison of PID controller with adaptive neuro-fuzzy controller is presented here. It is observed that the PID controller is incapable to maintain the commanded reference when the plant is subjected to windy conditions; the PID controllers also fail to cope with the variation in the dynamics of the Eight-Rotor MAV.

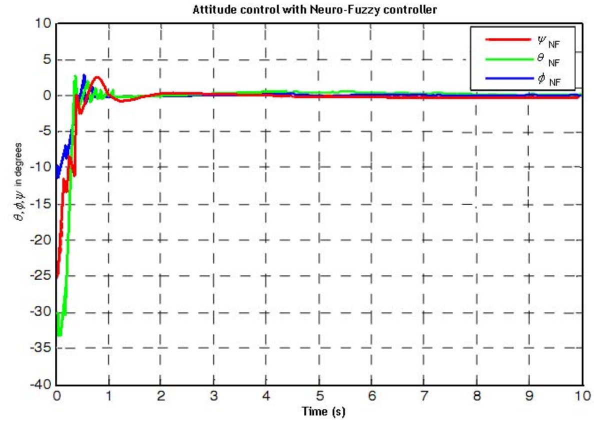

Fig. 6. Attitude control for Eight-Rotor MAV with Neuro-Fuzzy adptive controller without sensor noise.

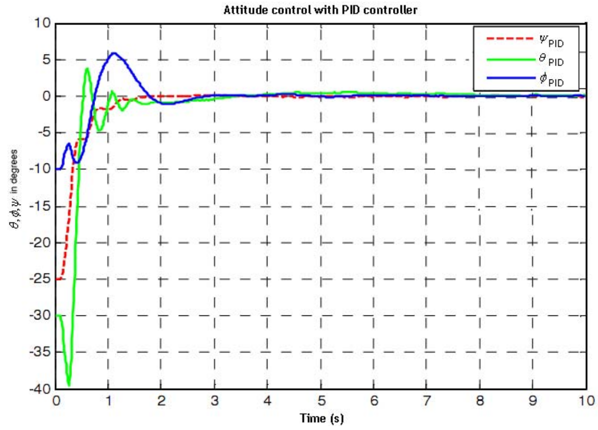

Fig. 7. Attitude control for Eight-Rotor MAV with PID controller without sensor noise.

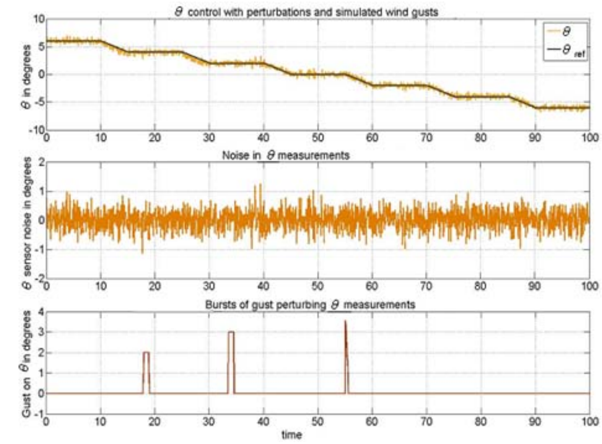

Fig. 8. Tracking a given angle in the presence of sensor noises and wind gusts.

Experimental results using adaptive neuro-fuzzy controller are compared with those from the PID controller for varied flight conditions and under the influence of external disturbance. To test the controller in experiments for robustness, the sensor noise and effects of gusts are included. An adaptive neuro-fuzzy based control system is designed for Eight-Rotor MAV with aid of the block diagram shown in Fig. 3. The yaw angle control performances by using neuro-fuzzy controller and PID controller have been shown in Figs. 6 and 7, from which we can see that the neuro-fuzzy controller performs faster than PID controller and has less overshoot. The sensor noise is a band limited white noise, whereas the vertical gusts are included in the form of small bursts at discrete times. A typical result for tracking a given angle in the presence of these two disturbances is shown in Fig. 8.

7. CONCLUSION

In this paper we have presented the dynamical modelling and intelligent control strategy of MAV having eight rotors. One of the main characteristics of these configurations is that the damage tolerance and increased stability in the wind. Two types of controller were presented for the Eight-Rotor MAV. One PID controller was derived in a conventional way, with simplified dynamics to reduce the number of higher-order derivative terms involved in the design process. This controller is not robust to uncertainty as well as sensor noise. As an alternative, we introduced a new robust control strategy which is achieved by using Neuro-Fuzzy adaptive controller, the Neuro-Fuzzy adaptive controller based on type-II fuzzy neural networks which is able to learn the inverse dynamics of the Eight-Rotor MAV on-line and reduce the tracking error to zero. The real-time experiments have shown an acceptable performace of the Eight-Rotor MAV applying the proposed control law.

REFERENCES

[1] P. Pounds, R. Mahony, and P. Hynes, "Design of a four-rotor aerial robot," *Proc. of Australian Conference on Robotics and Automation*, pp. 145-150, 2002.

[2] P. McKerrow, "Modelling the Draganflyer four-rotor helicopter," *Proc. of the IEEE International Conference on Robotics and Automation*, pp. 3596-3601, 2004.

[3] S. Bouabdallah, A. Noth, and R. Siegwart, "PID vs. LQ control techniques applied to an indoor Micro-Quadrotor," *Proc. of IEEE International Conference on Intelligent Robots and Systems*, vol. 14, pp. 2451-2456, 2004.

[4] A. Tayebi and S. McGilvray, "Attitude stablilization of a VIOL quadrotor aircraft," *IEEE Trans. on Control Systems Technology*, vol. 14, pp. 562-571, 2006.

[5] B. Erginer and E. Altug, "Modeling and PD control of a quadrotor VTOL vehicle," *Proc. of the IEEE Intelligent Vehicles Symposium*, pp. 894-899, 2007.

[6] D. Lee, H. J. Kim, and S. Sastry, "Feedback linearization vs. adaptive sliding mode control for a quadrotor helicopter," *International Journal of Control, Automation, and Systems*, vol. 7, no. 3, pp. 419-428, 2009.

[7] C. Coza and C. J. B. Macnab, "A new robust adaptive-fuzzy control method applied to quadrotor helicopter stabilization," *NAFIPS Annual meeting of the North American Fuzzy Information Society*, vol. 3, pp. 454-458, 2006.

[8] J. T. Spooner and M. Passino, "Stable adaptive control using fuzzy systems and neural networks," *IEEE Trans. on Fuzzy Systems*, vol. 3, pp. 339-359, 1996.

[9] R. Ordonez and K. Passino, "Stable multi-input multi-output adaptive fuzzy/neural control," *IEEE Trans. on Fuzzy Systems*, vol. 3, pp. 345-353, 1999.

[10] P. Melin and O. Castillo, "A new method for adaptive model-based control of non-linear dynamic plants using a neuro-fuzzy-fractal approach," *Soft Computing Journal*, vol. 2, pp. 171-177, 2001.

[11] X. Lou, Z. Sun, and F. Sun, "A new approach to fuzzy modeling and control for nonlinear dynamic systems: neuro-fuzzy dynamic characteristic modeling and adaptive control mechanism," *International Journal of Control, Automation, and Systems*, vol. 7, no. 1, pp. 123-132, 2009.

[12] P. Melin and O. Castillo, "Intelligent control of complex electrochemical systems with a neuro-fuzzy-genetic approach," *IEEE Trans. on Industrial Electronics*, vol. 5, pp. 951-955, 2001.

[13] M. J. Er, C. B. Low, K. H. Nah, M. H. Lim, and S. Y. Ng, "Real-time implementation of a dynamic fuzzy neural networks controller for a SCARA," *Microprocessors and Microsystems*, vol. 9-10, pp. 449-461, 2002.

[14] C. H. Lee, Y. C. Lin, and W. Y. Lai, "Systems identification using type-2 fuzzy neural network (type-2 FNN) systems," *Proc. IEEE Int. Symp. Comput. Intell. Robot. Autom.*, vol. 3, pp. 1264-1269, 2003.

[15] C. H. Wang, "Dynamic optimal training for interval type-2 fuzzy neural network (T2FNN)," *IEEE Trans. Syst., Man, Cybern. B*, vol. 3, pp. 1462-1477, 2004.

[16] X. J. Chen, D. Li, and Z. H. Xu, "Adaptive double axes motion control system based on Type-II fuzzy neural networks," *Optics and Precision and Engineering*, vol. 20, 2011.

[17] D. Li, X. J. Chen, Z. H. Xu, Y. Fan, and N. W. Da, "A type-II fuzzy neural networks with self-organizing recurrent intervals for dynamic time-varying system identification," *Optics and Precision and Engineering*, vol. 19, pp. 1406-1413, 2011.

[18] J. S. R. Jang, "ANFIS: adaptive-network-based fuzzy inference system," *IEEE Trans. on Systems, Man, and Cybernetics*, vol. 3, pp. 665-684, 1993.

Xiangjian Chen is a Ph.D. student at the Department of Mechanical and Electronic Engineering, Chang Chun Institute of Optics Fine Mechanics and Physics, Chinese Academy of Sciences, China. She received her Master degree at university of North East Dian Li. Her research interests include intelligent control and Micro aircraft vehicle.

Di Li studies embedded operation system and control, and he is a Ph.D. student at the Department of Mechanical and Electronic Engineering, Chang Chun Institute of Optics Fine Mechanics and Physics, Chinese Academy of Sciences, China. His interests include embedded operation system, image processing and Micro aircraft vehicle.

Yue Bai received his Ph.D. degree at the Department of Mechanical and Electronic Engineering, Chang Chun Institute of Optics Fine Mechanics and Physics, Chinese Academy of Sciences, China in 2006. His interests include automatic control and dynamics for MAV, and friction lubrication, space flywheel practical technology under extreme conditions.

Zhijun Xu is serving as Ph.D. supervisor and working at Chang Chun Institute of Optics Fine Mechanics and Physics, Chinese Academy of Sciences, China. His interests include automatic control and electronics.